Journal of Power Electronics, Vol. 16, No. 4, pp. 1407-1414, July 2016

JPE 16-4-17

http://dx.doi.org/10.6113/JPE.2016.16.4.1407
ISSN(Print): 1598-2092 / ISSN(Online): 2093-4718

An Improved Wavelet PWM Technique with Output Voltage Amplitude Control for Single-phase Inverters

Chun-Fang Zheng†, Bo Zhang*, Dong-Yuan Qiu*, Xiao-Hui Zhang*, and Rui Li**

†,**Department of Shipbuilding Engineering, Guangzhou Maritime Institute, Guangzhou, China
*Department of Electric Power, South China University of Technology, Guangzhou, China

Abstract

Unlike existing pulse-width modulation (PWM) techniques, such as sinusoidal PWM and random PWM, the wavelet PWM (WPWM) technique based on a Harr wavelet function can achieve a high fundamental component for the output voltage, low total harmonic distortion, and simple digital implementation. However, the original WPWM method lacks output voltage control. Thus, the practical application of the WPWM technique is limited. This study proposes an improved WPWM technique that can regulate output voltage amplitude with the addition of a parameter. The relationship between the additional parameter and the output voltage amplitude is analyzed in detail. Experimental results verify that the improved WPWM exhibits output voltage control in addition to all the merits of the WPWM technique.

Key words: Inverter, Total harmonic distortion (THD), Voltage modulation ratio, Wavelet modulation

I. INTRODUCTION

Inverters are important components of power electronic technology that are widely used in AC motor speed control, induction heating, uninterruptible power supply, and other fields. As a core aspect of inverters, the modulation strategy exerts a significant influence on the performance of inverters. A good control strategy can reduce harmonic pollution and switching losses and increase DC voltage utilization. At present, the commonly used modulation strategies [1]-[6] include sinusoidal pulse width modulation (SPWM), random pulse width modulation (RPWM), selective harmonic elimination, and a series of other optimization methods. Searching for an optimal control scheme to improve the output performance of inverters remains a critical research area [7]-[9].

In recent years, a wavelet modulation technique has been proposed for inverters [10]-[20]. Such wavelet modulation method is based on the Harr wavelet function and a non-dyadic multi-resolution analysis. The control signal generated by the wavelet modulation is a series of pulses with different widths. Therefore, this wavelet modulation technique is referred to as the wavelet PWM (WPWM) technique in the present work. In comparison with existing PWM techniques, such as the SPWM and RPWM techniques, the WPWM method is able to produce output voltage and current whose fundamental components exhibit higher magnitude; it also features lower total harmonic contents. However, the WPWM technique is not able to regulate the output voltage amplitude when the parameters are fixed.

Thus, we aim to analyze the feasibility of regulating the output voltage amplitude and propose an improved WPWM technique to realize the regulation of output voltage amplitude through the addition of a parameter. The rest of this paper is organized as follows. The basic theory of the WPWM technique is introduced in Section II. The improved WPWM technique is proposed in Section III. The experimental results are provided in Section IV. The conclusion is given in Section V.

II. FUNDAMENTALS OF THE WPWM TECHNIQUE

The WPWM technique is based on a sample and

Manuscript received Aug. 11, 2015; accepted Feb. 17, 2016
Recommended for publication by Associate Editor Bon-Gwan Gu.
†Corresponding Author: zcf219@163.com
Tel: +86-18138720358, Guangzhou Maritime Institute
*Dept. of Electric Power, South China University of Technology, China
**Dept. of Shipbuilding Eng., Guangzhou Maritime Institute, China

© 2016 KIPE

reconstruction of a reference-modulating signal in a non-uniform recurrent manner by using set sampling and synthesis basis functions [10]-[11]. These sampling basis functions are generated as dilated and translated versions of the scale-based linearly combined scaling function $\varphi_{(j,k)}(t)$. Furthermore, these synthesis basis functions are generated as dilated and translated versions of the scale-based linearly combined synthesis scaling function $\tilde{\varphi}_{(j,k)}(t)$. The scale-based linearly combined scaling function is defined at scale j as

$$\varphi_j(t)=\phi_H(2^{j+1}t)+\phi_H(2^{j+1}(t-1+2^{-(j+1)}))$$

and $$\varphi_{(j,k)}(t)=\varphi\left(2^j t-k\right) \quad (1)$$

where j = 0, 1, 2, 3, … and $\phi_H(t)$ is the Harr scaling function, which given by $\phi_H(t)=\begin{cases}1 & t\in[0,1]\\ 0 & t\notin[0,1]\end{cases}$.

The synthesis scaling function $\tilde{\varphi}(t)$ associated with $\varphi(t)$ can be defined as

$$\tilde{\varphi}_j(t)=(\phi_H)_j(t)-\varphi_j(t) \text{ and } \tilde{\varphi}_{(j,k)}(t)=\tilde{\varphi}\left(2^j t-k\right) \quad (2)$$

Using these two dual scaling functions, we can expand a continuous time signal $x_c(t)$ as

$$x_c(t)=\sum_k\sum_j\left\langle x_c(t),\varphi\left(2^j t-k\right)\right\rangle\tilde{\varphi}\left(2^i t-k\right) \quad (3)$$

where $j, k \in$ Z, and Z represent a set of integer numbers.

Such form of signal processing suggests that a continuous time signal $\left\langle x_c(t),\varphi\left(2^j t-k\right)\right\rangle$ can be recovered from its samples using sets of synthesis functions $\tilde{\varphi}\left(2^j t-k\right)$.

The literature [10] proves that the switching pulses for inverters can be generated by using dilated and shifted versions of the synthesis scaling function $\tilde{\varphi}_{(j,k)}(t)$. When each cycle of $x_c(t)$ is divided by a finite number of sample groups D, the length of the time interval of the sample group [t_{d1}, t_{d2}] changes as scale j changes. That is,

$$t_{d1}=d+2^{-j-1}$$
$$t_{d2}=d+1-2^{-j-1} \quad \text{and } d=0,1,2,\cdots,(D-1) \quad (4)$$

Generally, the sampled signal for a single-phase inverter is a sinusoidal one $S_M(t)=\sin(\omega_m t)$ with a period of T_m, which exhibits quarter-cycle symmetry. The procedure of the WPWM technique given in the literature [10] shows that the output voltage of an inverter mainly depends on the initial value of scale j (j0) and the number of sample groups (D) in a period.

When turning switching devices on and off at time points (t_{d1} and t_{d2}), a voltage pulse waveform can be obtained. Thus, according to the Fourier analysis, the amplitude of the k^{th} harmonic voltage V_k can be defined as

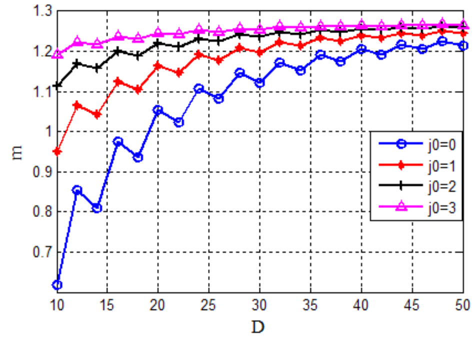

Fig. 1. m vs. D when j_0 = 0, 1, 2, 3.

$$V_k=\frac{2V_{dc}}{k\pi}\times\sum_{d=0,j=j0}^{D-1}\left[\cos\left(k(d+1-2^{-j-1})*\frac{2\pi}{D}\right)-\cos\left(k(d+2^{-j-1})*\frac{2\pi}{D}\right)\right] \quad (5)$$

where $k=1,3,5,7,\cdots$, V_{dc} is the amplitude of the input DC voltage for inverters, and V_1 is the amplitude of fundamental voltage.

The voltage modulation ratio of an inverter is defined as $m=V_1/V_{dc}$; from (5), m can be determined by

$$m=\frac{4}{\pi}\left[\sum_{d=0,j=jo}^{D-1}\sin\left[(d+0.5)*\frac{2\pi}{D}\right]\sin\left(\frac{1-2^{-j}}{2}*\frac{2\pi}{D}\right)\right] \quad (6)$$

From (6), the value of m under different initial values of scale can be calculated via MATLAB. The results of m vs. D when j0 = 0, 1, 2, 3 are shown in Fig. 1. As shown in the figure, m increases as j0 increases under the same D, and m increases as D increases under the same j0. However, once D and j0 are fixed, m is determined. Thus, the inverter controlled by the WPWM method lacks output voltage amplitude control, which is a flaw of the WPWM method for many applications.

III. IMPROVED WPWM TECHNIQUE

A. Principle of the Improved WPWM Technique

The output of inverters can be controlled in many ways, one of which is the use of pulse-width modulation (PWM). The principle of PWM is to control the output voltage amplitude of inverters by varying the widths of the pulses. The control signals for inverters generated by the WPWM technique are a type of PWM signal, and the width of the control signals when D and j0 are fixed is determined. Hence, the WPWM technique lacks output voltage amplitude control. Varying the widths of the pulses generated by the WPWM technique when D and j0 are given obviously deserves research attention.

According to (4), if a new parameter μ is added to calculate the time interval of a sample group, then the width of the pulses can be adjusted. As d represents the sampling group, the new parameter μ may be added in four ways:

Method 1: $t_{d1} = d + 2^{-(\mu * j+1)}$, $t_{d2} = d + 1 - 2^{-(\mu * j+1)}$;
Method 2: $t_{d1} = d + 2^{-\mu * (j+1)}$, $t_{d2} = d + 1 - 2^{-\mu * (j+1)}$;
Method 3: $t_{d1} = d + \mu * 2^{-(j+1)}$, $t_{d2} = d + 1 - \mu * 2^{-(j+1)}$;
Method 4: $t_{d1} = d + \mu * 2^{-(j+1)}$, $t_{d2} = d + \mu * [1 - 2^{-(j+1)}]$.

The original WPWM can be considered as a special case when $\mu = 1.0$.

The comparison of **Methods 1–4** is discussed on the basis of the following aspects:

(1) Pulse width, i.e., the value of t_{d2}-t_{d1}. As t_{d2}-$t_{d1} \geq 0$ must be satisfied, $\mu * j \geq 0$ is required for **Method 1**, $\mu*(j+1) \geq 1$ is required for **Method 2**, $\mu \leq 2^{j}$ is required for **Method 3**, and $\mu*(1\text{-}2^{-j}) \geq 0$ is required for **Method 4**. Given that $j \geq 0$, the value of μ when j is given can be easily determined. Further study reveals that $0 \leq \mu \leq 1$ can be satisfied in **Methods 1 and 4** when the voltage modulation ratio m is regulated from 0 to its maximum. However, the value of μ in **Methods 2 and 3** changes into j, which makes the choice of μ considerably difficult for different output voltage amplitudes.

(2) Complexity of the algorithm. Obviously, the complexity of **Method 1** and the difficulty involved in its digital implementation increase because the power of 2 is not a constant when $0 \leq \mu \leq 1$.

Thus, **Method 4** is selected to regulate the width of the pulses. The algorithm for implementing the improved WPWM technique with **Method 4** is set up according to the literature [20]. Its flowchart is shown in Fig. 2, where $T_m = 1/f_m$ is the period of the modulating sinusoidal signal and $t_{d3} = t_{d2|\mu=1.0}$ is used to determine the value of j and thereby ensure that similar to those in the original WPWM, the output waveforms exhibit quarter-cycle symmetry.

B. Analysis of the Improved WPWM Technique

In **Method 4,** the pulse width changes to t_{d2}- $t_{d1} = \mu*(1 - 2^{-j})$. Then, m is expressed by

$$m = \frac{4}{\pi}\left[\sum_{d=0, j=j0}^{D-1} \sin\left[(d+\frac{\mu}{2})*\frac{2\pi}{D}\right]\sin(\mu*\frac{1-2^{-j}}{2}*\frac{2\pi}{D})\right] \quad (7)$$

According to (7), m decreases as μ decreases when choosing $0 \leq \mu \leq 1$. Thus, the output voltage amplitude can be controlled by changing the parameter μ.

To determine the relationship between the parameter μ and the output voltage amplitude of inverters, $f_m = 50$ Hz, $D = 30$, and j0 = 0 are selected; μ is changed in step 0.01 from 0.01 to 1; and the voltage modulation ratio m of the inverter is calculated on the basis of (7). The curve of m vs. μ is illustrated in Fig. 3. The curve resembles a straight line. By fitting the curve with a linear function [21]-[22], the fitting result is derived as $m = 0.0008 + 1.1223*\mu$, and the fitting errors are shown in Fig. 4. As shown in the figure, the fitting error is less than 8×10^{-4}, which is too small to be neglected.

In this work, a single-phase full-bridge (FB) inverter is selected as an example. The input voltage $V_{dc} = 100\text{V}$, the output frequency $f_m = 50$ Hz, $D = 30$, and j0 = 0. The simulation results of the output voltage and its spectrum for $\mu = 0.8$ and $\mu = 0.9$ are shown in Fig. 5. The simulated output voltage amplitudes are close to the theoretical values $m = 0.0008+1.1223*0.8 = 0.8986$ when $\mu = 0.8$ and $m = 0.0008+1.1223*0.9 = 1.0109$ when $\mu = 0.9$. This result proves that the inverter output voltage amplitude can be regulated by parameter μ.

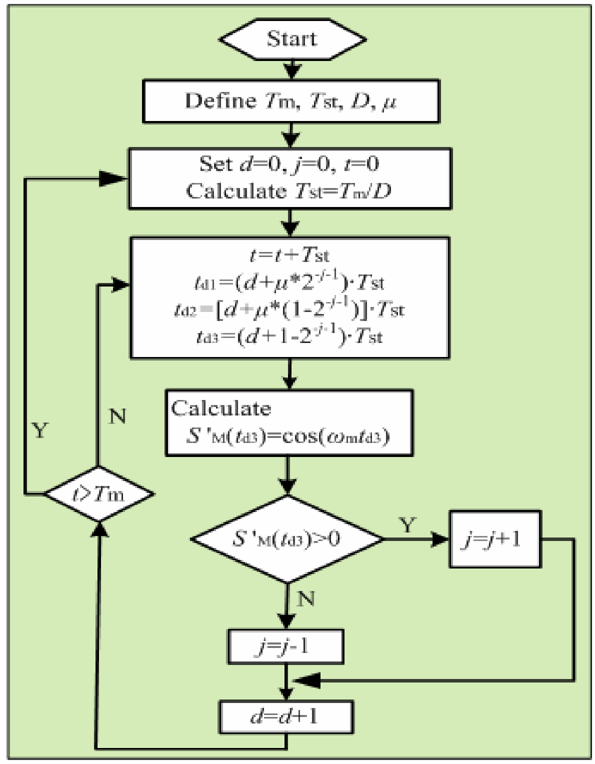

Fig. 2. Flowchart of the improved WPWM technique.

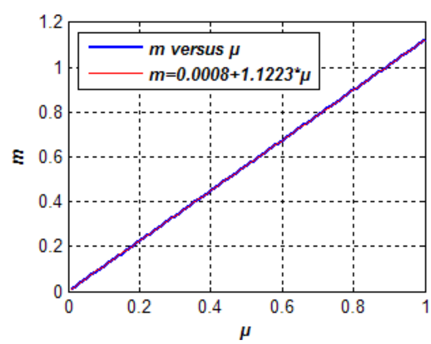

Fig. 3. m vs. μ.

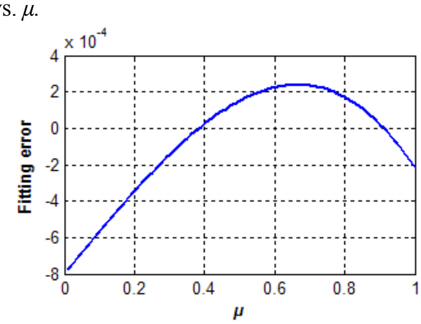

Fig. 4. Fitting errors.

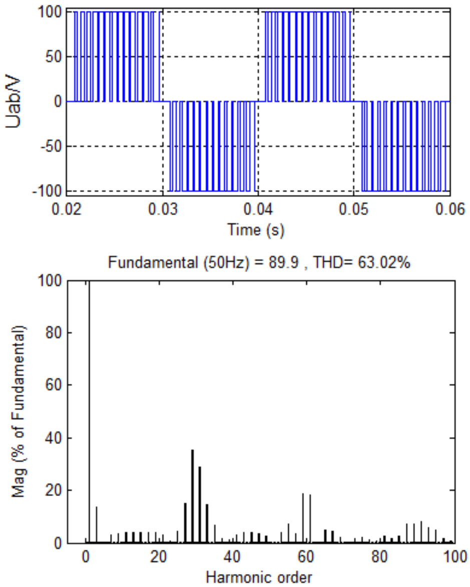

(a) $\mu = 0.8$.

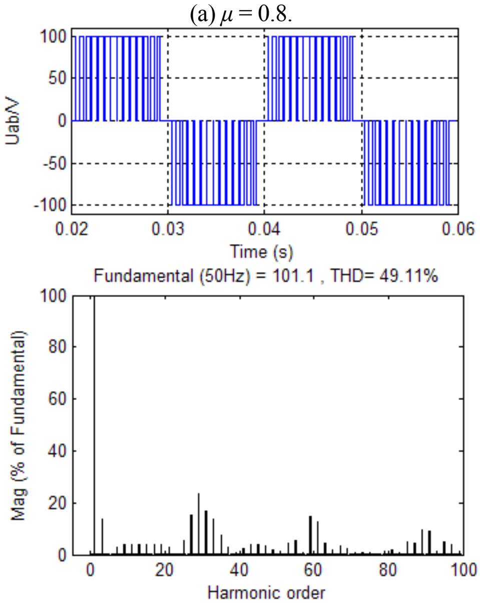

(b) $\mu = 0.9$.

Fig. 5. Simulation results of the output voltage and its spectrum at different μ .

TABLE I

FITTING FUNCTION M = F(M) FOR DIFFERENT D

D	$m = f(\mu)$
20	$m = 1.0679*\mu+0.0008$
22	$m = 1.0219*\mu+0.0008$
24	$m = 1.1178*\mu+0.0008$
26	$m = 1.0806*\mu+0.0008$
28	$m = 1.1527*\mu+0.0008$
30	$m = 1.1223*\mu+0.0008$
32	$m = 1.1777*\mu+0.0008$
34	$m= 1.1525*\mu+0.0006$
36	$m = 1.1960*\mu+0.0006$
38	$m = 1.1747*\mu+0.0006$
40	$m = 1.2097*\mu+0.0005$

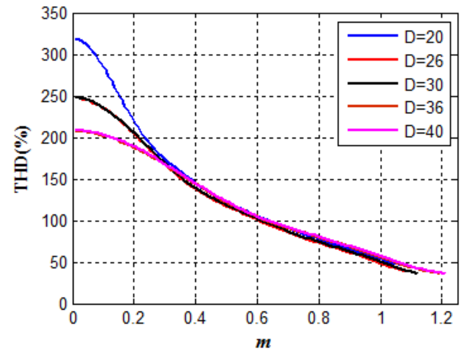

Fig. 6. THD vs. m at different D.

Similarly, the relationship between μ and m can be derived by a series of fitting equations for different D. The fitting function $m = f(\mu)$ at $f_m = 50$ Hz and j0=0 for different D when the fitting error is controlled to be less than 8×10^{-4} is presented in Table I. The calculation results of the total harmonic distortion (THD, total of the former 101th harmonics) vs. m for different D are shown in Fig. 6. The figure clearly shows that THD decreases as m increases.

IV. EXPERIMENTAL RESULTS

To verify the improved WPWM technique, we implement the algorithm of the improved WPWM technique by using a digital signal processor (TMS320F28335). The input voltage (U_{in}) of the prototype is $U_{in} = 50$ V. MOSFET IRF450 is selected as a switch, TLP250 is used as a driver, and resistor $R = 50\ \Omega$ is used as the load. The experiments are carried out by choosing $m = 0.8$ and $\mu = 1$ (the values of m and μ are calculated with the expression in Table I) when j0 = 0, $f_m = 50$ Hz, and D = 26, 30, 36, 40. The experimental results of the output voltage U_{ab} and its spectrum are shown in Figs. 7–10, which show that the spectrum of U_{ab} is the *rms* (root mean square) value of different orders of harmonic voltage. As V_1 ($V_1 = m*V_{dc}$) is the amplitude of fundamental voltage, the theoretical *rms* value of the fundamental voltage is defined by $V_{1rms} = m*V_{dc}/\sqrt{2}$. For example, the theoretical *rms* value of the fundamental component of the inverter output voltage at $m = 0.8$ is close to $50*0.8/\sqrt{2} = 28.3$ V. The experimental results and the corresponding theoretical *rms* values for different D are listed in Table II.

Table II shows that the derived fitting equation $m = f(\mu)$ for different D is feasible because the error between the theoretical *rms* value and the experimental value is very small and the improved WPWM technique can regulate the output voltage amplitude of inverters with an extra parameter μ, in addition to all the merits of the WPWM technique.

To test the regulation ability of the improved WPWM technique, we design a digital control scheme with a voltage feedback loop for a single-phase FB inverter (Fig. 11). The experimental setup is shown in Fig. 12. The experiments are

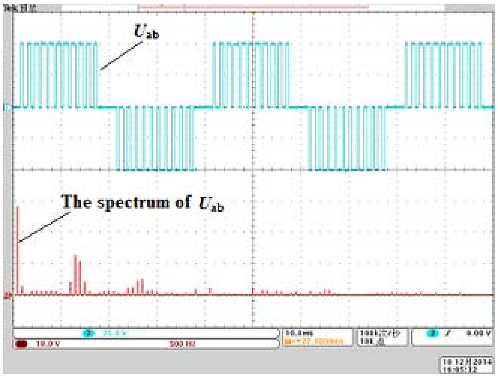

(a) $m = 0.8$ ($\mu = 0.7396$).

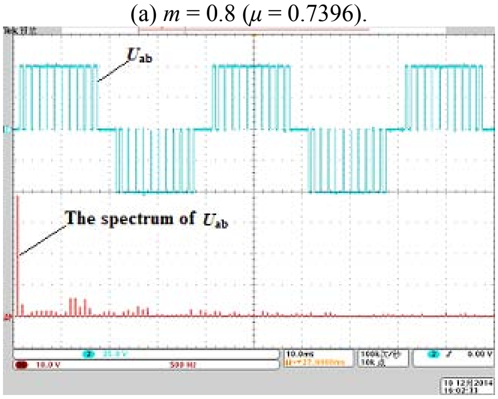

(b) $m = 1.0814$ ($\mu = 1$).

Fig. 7. Output voltage and its spectrum for a single-phase FB inverter with the improved WPWM at $j_0 = 0$, $D = 26$, and $f = 50$ Hz.

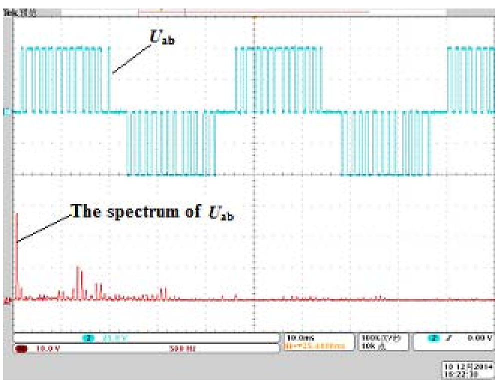

(a) $m = 0.8$ ($\mu = 0.7121$).

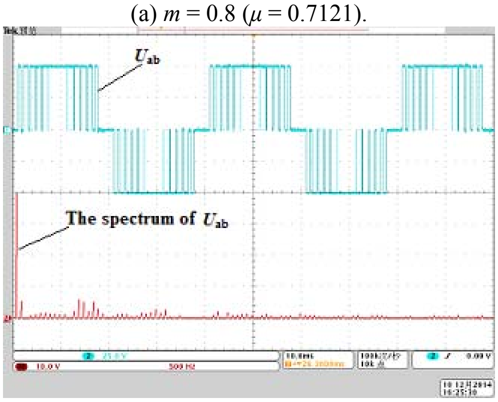

(b) $m = 1.123$ ($\mu = 1$).

Fig. 8. Output voltage and its spectrum for a single-phase FB inverter with the improved WPWM at $j_0 = 0$, $D = 30$, and $f = 50$ Hz.

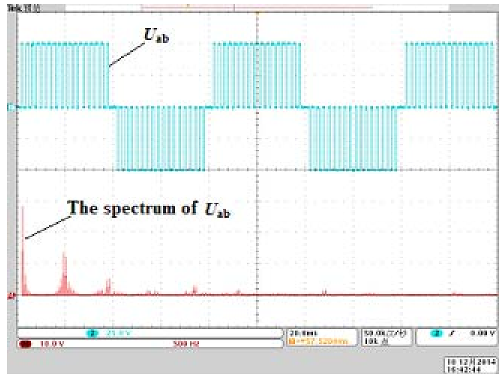

(a) $m = 0.8$ ($\mu = 0.6684$).

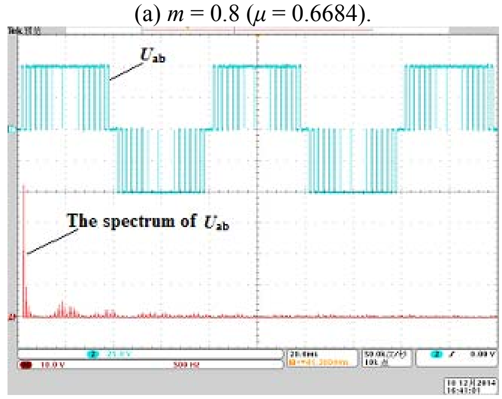

(b) $m = 1.1966$ ($\mu = 1$).

Fig. 9. Output voltage and its spectrum for a single-phase FB inverter with the improved WPWM at $j_0 = 0$, $D = 36$, and $f = 50$ Hz.

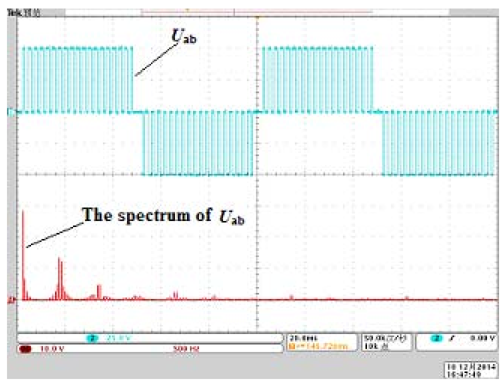

(a) $m = 0.8$ ($\mu = 0.6609$).

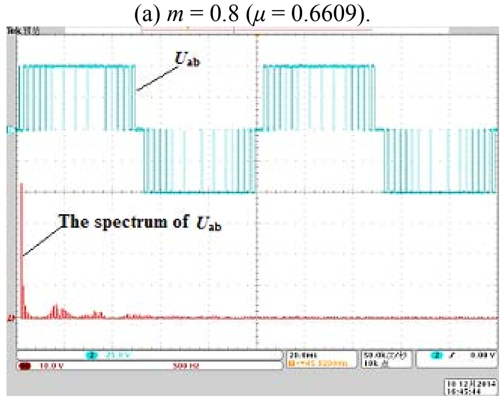

(b) $m = 1.2102$ ($\mu = 1$).

Fig. 10. Output voltage and its spectrum for a single-phase FB inverter with the improved WPWM at $j_0 = 0$, $D = 40$, and $f = 50$ Hz.

TABLE II
EXPERIMENTAL RESULTS FOR DIFFERENT D

D	*m*	Theoretical *rms* value	Experimental value
26	$m = 0.8$ ($\mu = 0.7396$)	28.3 V	28.2 V
	$m = 1.0814$ ($\mu = 1$)	38.2 V	38.4 V
30	$m = 0.8$ ($\mu = 0.7121$)	28.3 V	28 V
	$m = 1.123$ ($\mu = 1$)	39.7 V	40 V
36	$m = 0.8$ ($\mu = 0.6684$)	28.3 V	28.4 V
	$m = 1.1966$ ($\mu = 1$)	42.3 V	42.2 V
40	$m = 0.8$ ($\mu = 0.6609$)	28.3 V	28.4 V
	$m = 1.2102$ ($\mu = 1$)	42.8 V	42.8 V

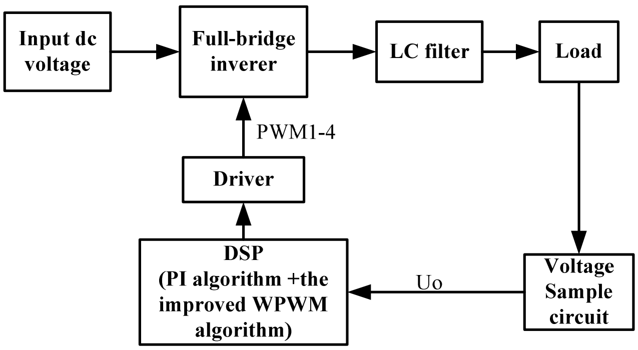

Fig. 11. Digital control scheme with voltage feedback loop.

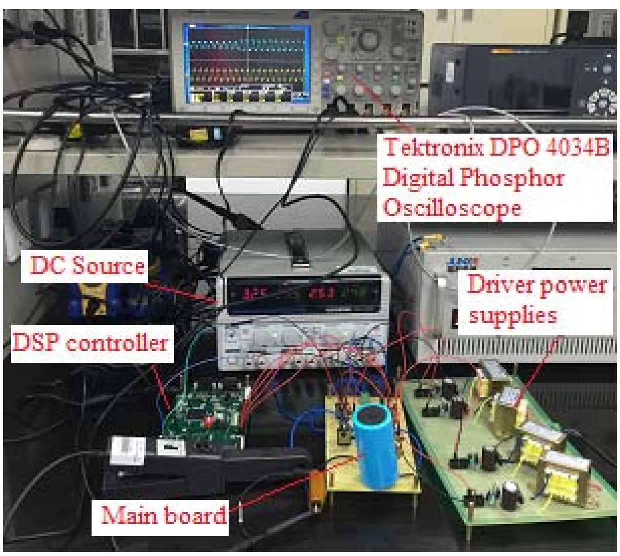

Fig. 12. Experimental platform.

carried out by choosing j0 = 0, fm = 50 Hz, and D = 30; the reference voltage (Vref) for the output voltage (Uo) is set to 28 Vrms (40 Vmax) and 35 Vrms (50 Vmax). The experimental waveforms when Vref = 28 Vrms and Vref = 35 Vrms after changing the input voltage from 40 V to 50 V or from 50 V to 40 V are shown in Figs. 13 and 14, respectively. The experimental waveforms when Vref = 28 Vrms and Vref = 35 Vrms after changing the load from 50 Ω to 27 Ω or from

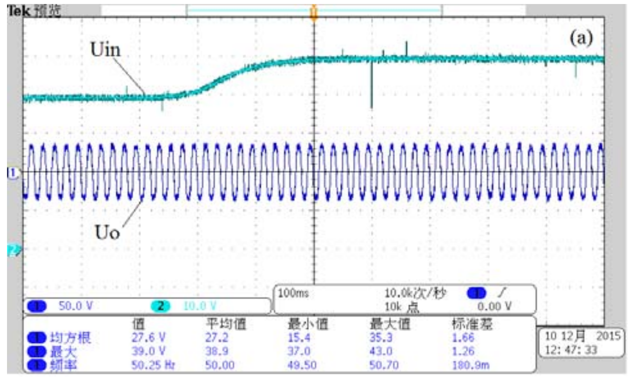

(a) Input voltage is changed from 40 V to 50 V.

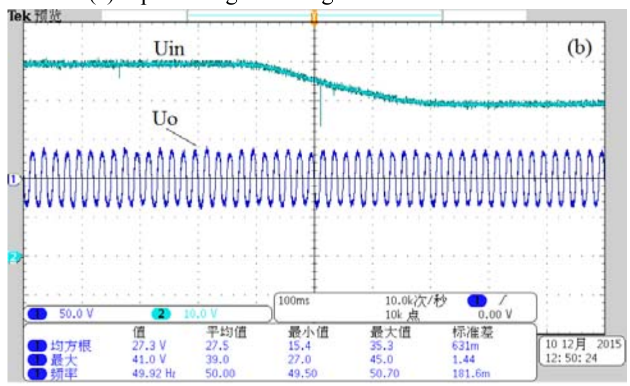

(b) Input voltage is changed from 50 V to 40 V.

Fig. 13. Input and output voltages when the reference voltage is 28 Vrms.

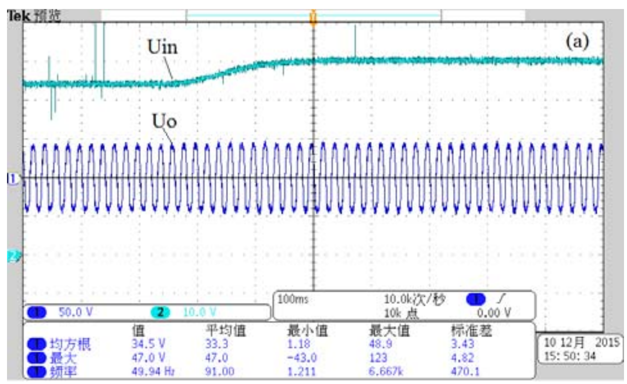

(a) Input voltage is changed from 40 V to 50 V.

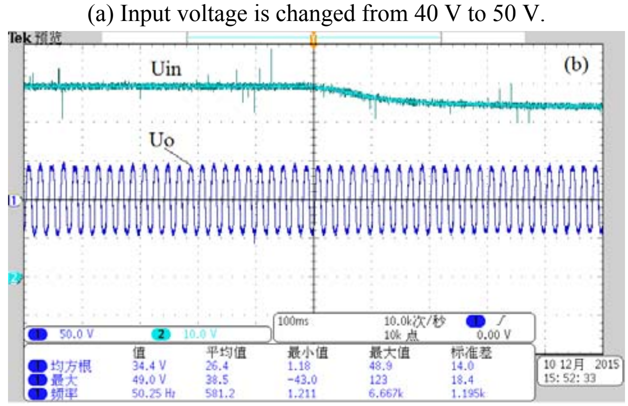

(b) Input voltage is changed from 50 V to 40 V.

Fig. 14. Input and output voltages when the reference voltage is 35 Vrms.

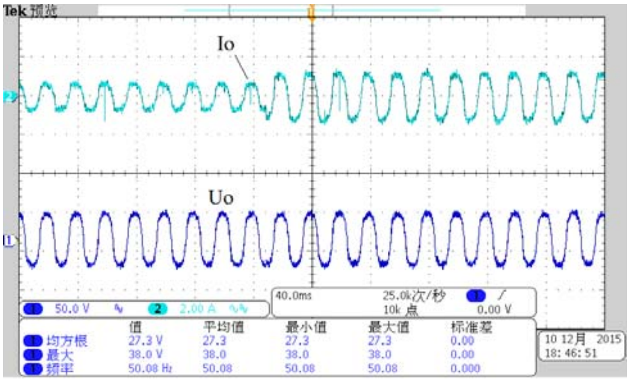

(a) Load is changed from 50 Ω to 27 Ω.

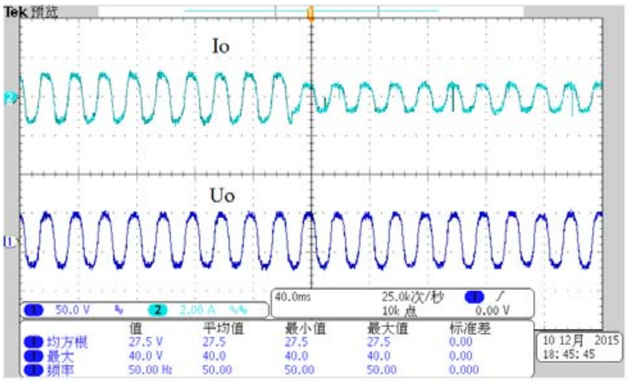

(b) Load is changed from 27 Ω to 50 Ω.

Fig. 15. Load current and output voltage when the reference voltage is 28 Vrms.

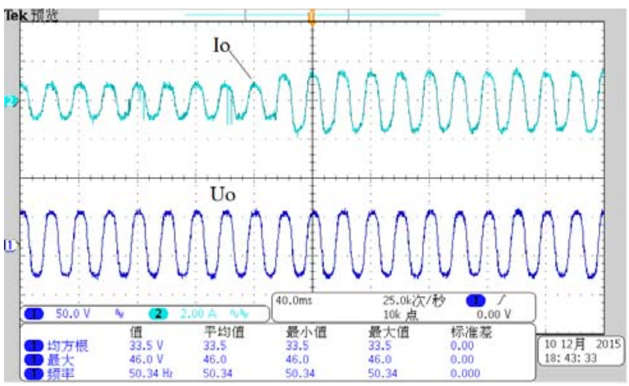

(a) Load is changed from 50 Ω to 27 Ω.

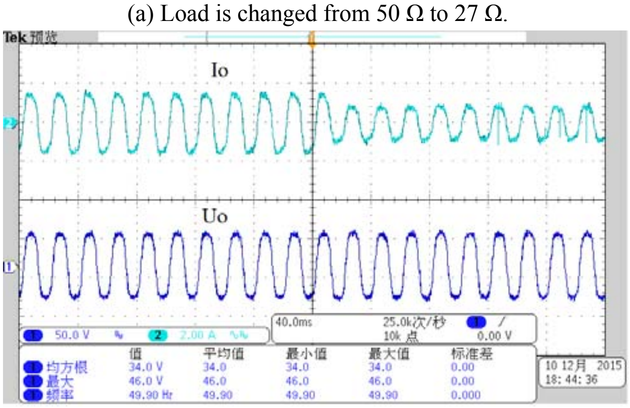

(b) Load is changed from 27 Ω to 50 Ω.

Fig. 16. Load current and output voltage when the reference voltage is 35 Vrms.

27 Ω to 50 Ω are shown in Figs. 15 and 16, respectively. Fig. 13 shows that the output voltage can be stable when *m* is changed between 0.8 and 1. Fig. 14 shows that the output voltage can be stable when *m* is changed between 1 and 1.11. Figs. 15–16 show that the output voltage can be regulated to a stable value quickly.

V. Conclusions

This work analyzes the feasibility of modifying the WPWM technique based on the Harr wavelet function and proposes an improved WPWM technique to realize output voltage regulation through an extra parameter. The relationship between the additional parameter and the output voltage amplitude for different numbers of sample groups can be represented by a group of linear functions. The experimental results for a single-phase FB inverter prove that the improved WPWM technique can regulate the output voltage amplitude linearly through the additional parameter with simple digital implementation, which is beneficial for inverters that require constant output voltage in a constant frequency.

Acknowledgment

This research was supported in part by the Key Program of the National Natural Science Foundation of China under Grant 51437005, the National Natural Science Foundation of China 51277079, and the Guangdong Public Welfare Research and Capacity Building Foundation (2015A010103024).

References

[1] S. R. Bowes and P. R. Clark, “Simple microprocessor implementation of new regular- sampled harmonic elimination technique,” *IEEE Trans. Ind. Appl.*, Vol. 28, No. 1, pp. 89-95, Jan./Feb. 1992.

[2] B. N. Chaudhari and B. G. Femandes, “EPROM-based modulator for synchronized asymmetric regular-sampled SPWM technique,” in *Proceedings of IEEE International Conference on Industrial Technology 2000*, Vol. 2, pp. 278-283, Jan. 2000.

[3] J. Chiasson, L. M. Tolbert, K. McKenzie, and Z. Du, “A complete solution to the harmonic elimination problem,” in *18th Annual IEEE Applied Power Electronics Conference and Exposition(APEC)*, Vol. 1, pp. 596-602, Feb. 2003.

[4] G. Narayanan, D. Zhao, H. K. Krishnamurthy and R. Ayyanar, “Space vector based hybrid PWM techniques for reduced current ripple,” *IEEE Trans. Ind. Electron.*, Vol. 55, No. 4, pp. 1614-1627, Apr. 2008.

[5] H. Khan, E. H. Miliani, H. Ouzaarou, and K. E. K. Drissi, “Random discontinuous space vector modulation for variable speed drives,” in *IEEE International Conference on Industrial Technology (ICIT)*, pp. 985-990, Mar. 2012.

[6] R. Salehi, N. Farokhnia, M. Abedi, and S. H. Fathi, “Elimination of low order harmonics in multilevel inverter using genetic algorithm,” *Journal of Power Electronics*, Vol. 11, No. 2, pp. 132-139, Mar. 2011.

[7] Z. Li, P. Wang, H. Zhu, Z. Chu, and Y. Li, “An improved pulse width modulation method for chopper-cell-based

multilevel inverters," I*EEE Trans. Power Electron.*, Vol. 27, No. 8, pp. 3472–3481, Aug. 2012.

[8] A. Marzoughi, H. Imaneini, and A. Moeini, "An optimal selective harmonic mitigation technique for high power converters," *International Journal of Electrical Power and Energy Systems*, Vol. 49, pp. 34-39, Jul. 2013.

[9] M. Zhang, L. Huang, W. Yao, and Z. Lu. "Circulating harmonic current elimination of a CPS-PWM-based modualr mulitlevel converter with a plug-in repetitive controller," *IEEE Trans. Power Electron.*, Vol. 29, No. 4, pp. 2083–2097, Apr. 2014.

[10] S. A. Saleh, C. R. Moloney, and M. A. Rahman, "Developing a nondyadic MRAS for switching DC–AC inverters," in *Digital Signal Processing Workshop*, pp.544–549, Sep. 2006.

[11] S. A. Saleh, C. R. Moloney, and M. A. Rahman, "Development and testing of wavelet modulation for single-phase inverters," *IEEE Trans. Ind. Electron.*, Vol. 56, No. 7, pp. 2588–2599, Jul. 2009.

[12] S. A. Saleh and M. A. Rahman, "Development and testing of a new controlled wavelet modulated inverter for IPM motor drives," *IEEE Trans. Ind. Appl.*, Vol. 46, No. 4, pp. 1630–1643, Jul./Aug. 2010.

[13] S. A. Saleh, C. R. Moloney, and M. A. Rahman, "Analysis and development of wavelet modulation for three phase voltage source inverters," *IEEE Trans. Ind. Electron.*, Vol. 58, No. 8, pp. 3330–3348, Aug. 2011.

[14] S. A. Saleh and M. A. Rahman, "Development and experimental validation of resolution-level controlled wavelet modulated inverters for three phase induction motor drives," *IEEE Trans. Ind. Appl.*, Vol. 47, No. 4, pp. 1958–1970, Jul./Aug. 2011.

[15] S. A. Saleh, "The implementation and performance evaluation of 3φVS wavelet modulated ac-dc converters," *IEEE Trans. Power Electron.*, Vol. 28, No. 3, pp. 1096–1106, Mar. 2013.

[16] R. Adlakha and P. R. Sharma, "Space vector modulation for two level and three level VSI and comparison with wavelet modulation," in *Proceeding of 4th International Conference (IRAJ)*, pp. 57-62, Dec. 2013.

[17] J. Zhang, Y. Wei, X. Li, and H. Qi. "Inverter control technology based on multi-resolution wavelet modulation," in *IEEE Conference and Expo Transportation Electrification Asia-Pacific (ITEC Asia-Pacific)*, pp. 1-5, Aug./Sep. 2014.

[18] U Laishram and A. M. Nagaraj, "Wavelet modulation for neutral point clamped multilevel inverters," *International Journal of Emerging Technology and Advanced Engineering*, Vol. 4, No. 3, pp. 61-65, Mar. 2014.

[19] C.-F. Zheng, B. Zhang, D.-Y. Qiu, X.-H. Zhang, and L.-M. Xiao, "Wavelet PWM technique for single-phase three-level inverters," *Journal of Power Electronics*, Vol. 15, No. 6, pp. 1517-1523, Nov. 2015.

[20] C. F. Zheng, X. M. Xu, B. Zhang, and D. Y. Qiu, "Inverter's characteristic analysis under different parameters of wavelet PWM technique," in *16th European Conference on Power Electronics and Applications* (*EPE'14-ECCE* Europe), pp.1-7, Aug. 2014.

[21] C. Zheng, B. Zhang, and D. Qiu, "Digital natural sampling SPWM based on inverse operator method," in *IEEE Power Electronics Specialists Conference*(*PESC)*, pp. 792-797, Jun. 2007.

[22] Q. Jiang, D. G. Holmes, and D. B. Giesner, "Method for linearising optimal PWM switching strategies to enable their computation on-line in real-time," in *IEEE Industry Applications Society Annual Meeting*, Vol. 1, pp. 819-825, Sep./ Oct. 1991.

Chun-Fang Zheng was born in China, in 1978. She received her B.S. degree in Electrical Engineering from Nanchang University, Jiangxi, China, in 2000, an her M.S. and Ph.D. degrees from South China University of Technology, Guangzhou, China, in 2003 and 2006, respectively. From 2006 to 2010, she was an Engineer Supervisor in Emerson Network Power ASTEC Power Supply (Shenzhen) Co., Ltd., China. Since 2013, she has been an associate Professor in the School of Shipbuilding Engineering, Guangzhou Maritime Institute, China. Her main research interests include the design and control of power converters and inverters.

Bo Zhang was born in Shanghai, China, in 1962. He received his B.S. degree from Zhejiang University, Hangzhou, China, in 1982; his M.S. degree from Southwest Jiaotong University, Chengdu, China, in 1988; and his Ph.D. degree from Nanjing University of Aeronautics and Astronautics, Nanjing, China, in 1994. He is currently a Professor and the Vice Dean of the School of Electric Power, South China University of Technology, Guangzhou, China. He has authored or coauthored more than 400 papers and 2 books in Wiley. He also holds 24 patents. His current research interests include nonlinear analysis and control of power electronics and ac drives.

Dong-Yuan Qiu was born in China, in 1972. She received her B.S. and M.S. degrees from South China University of Technology, Guangzhou, China, in 1994 and 1997, respectively, and her Ph.D. degree from the City University of Hong Kong, Kowloon, Hong Kong, in 2002. Since 2010, she has been a Professor in the School of Electric Power, South China University of Technology. Her main research interests include the design and control of power converters, fault diagnosis, and sneak circuit analysis of power electronic systems.

Xiao-Hui Zhang was born in Fujian, China. She received her B.S. degree from Xiamen University, Xiamen, China, in 2014. She is currently working toward her M.S. degree in Power Electronics in South China University of Technology, Guangzhou, China. Her research interest is wavelet modulation.

Rui Li was born in Hebei, China, in 1979. He received his B.S. degree from Hebei University of Science and Technology, Shijiazhuang, China, in 2001; his M.S. degree from Korea Maritime University, Busan, Korea, in 2005; and his Ph.D. degree from Korea Maritime University, Busan, Korea, in 2007. He is currently an Associate Professor in Guangzhou Maritime Institute, Guangzhou, China. His research interests include smart grid and control of power electronics.